

***Ab initio* thermodynamics beyond the quasiharmonic approximation: W as a prototype**

Shikai Xiang,^{*} Feng Xi, Yan Bi, Ji'an Xu, Huayun Geng, Lingcang Cai, and Fuqian Jing
*National Key Laboratory of Shock Wave and Detonation Physics, Institute of Fluid Physics, P.O. Box 919-111,
 Mianyang, Sichuan 621900, China*

Jing Liu

Institute of High Energy Physics, Chinese Academy of Sciences, Beijing 100049, China

(Received 15 September 2009; revised manuscript received 5 November 2009; published 11 January 2010)

We present a simple but accurate scheme to compute the thermodynamic properties of crystalline solids in a wide range of pressure and temperature based on *ab initio* calculations. Compared to the method based on *ab initio* thermodynamic-integration techniques, our approach can reduce dramatically the number of *ab initio* molecular-dynamics simulations needed in the calculations of the intrinsic anharmonic effect neglected in the conventional quasiharmonic approximation. Taking tungsten as an example, we show that its thermal properties including the linear thermal-expansion coefficient and the equation of state (EOS) at high pressures and temperatures can be calculated accurately. The precise EOS of W for the pressure up to 500 GPa and the temperature up to 10 000 K may serve as a pressure scale. This method may be able to be extended to the study of solid-solid phase transitions of various crystalline solids, including some alloys.

DOI: [10.1103/PhysRevB.81.014301](https://doi.org/10.1103/PhysRevB.81.014301)

PACS number(s): 65.40.-b, 64.30.-t, 05.70.-a

I. INTRODUCTION

Parameter-free *ab initio* techniques based on density-functional theory (DFT) have been widely used to predict material properties, including thermodynamic properties.¹ Those most accurate *ab initio* thermodynamic calculations of crystalline solids at high temperatures are usually based on the quasiharmonic approximation,² the particle-in-a-cell (PIC) model^{3,4} or the thermodynamic-integration techniques combined with direct *ab initio* molecular-dynamics (AIMD) simulations.^{5,6}

In the quasiharmonic approximation, the lattice vibrations at each volume are harmonic and the phonon-dispersion relations (PDRs) relate only to the corresponding volume, not directly to the temperature. The phonon frequencies are functions of the temperature only through their volume dependence. The PDRs at high temperatures and various volumes are usually calculated at zero temperature, and the effects from electron excitation on the PDRs are neglected. Meanwhile, the phonon interactions, resulted from the high-order terms of the interaction potential among the ions, are ignored. The quasiharmonic approximation has been shown to be able to reproduce the thermodynamic properties^{7,8} and thermal elasticity⁹ of solids at very high temperature. Even so, the intrinsic anharmonic effects (all the effects neglected by the conventional quasiharmonic approximation) on the thermal properties will gradually become profound at the temperatures approaching the melting point.

The PIC model is the second approximate way to evaluate the vibrational contribution to the Helmholtz free energy. In the PIC model (see, for example, Refs. 10–12), each atom is assumed to displace in its Wigner-Seitz cell in the potential field contributed from all the other atoms fixed at their equilibrium positions. The partition function and hence the free energy is calculated via an integration over the displacement of a single atom from its equilibrium position inside the Wigner-Seitz cell. Thus the $3N$ -dimensional integration in the partition function is reduced to a simple three-

dimensional integration. The PIC model is essentially an anharmonic Einstein model. Its advantage over lattice dynamics based on the quasiharmonic approximation is that all the high-order terms besides quadratic term of the interaction potential among the ions have been included exactly without a perturbation expansion in the calculations of thermal properties. But, on the other hand, the interatomic correlations between the motions of different atoms are ignored, thereby it is only valid at high temperatures above the Debye temperature. At low temperatures below the Debye temperature, the interatomic correlations cannot be neglected and the PIC model fails.

The last approach, which combines the thermodynamic-integration techniques with direct AIMD simulations, has also been used more frequently to calculate the thermodynamic properties of solids and liquids.^{5,6} For convenience, we call it *ab initio* thermodynamic-integration (AITI) method. The basis of the AITI method is to obtain the free-energy difference between a reference system, whose free energy can be calculated easily, and the *ab initio* system by thermodynamic integration following a specially designed reversibly and isothermally path in which the interactions among the ions are switched gradually from that of the reference system to that of the *ab initio* system by changing the mixture ratio of the two interactions. The practical feasibility of calculating *ab initio* free energies of liquids and anharmonic solids depends on finding a reference system whose free energy is readily calculated and the total-energy difference of the reference system and *ab initio* system is very small.¹³ The thermal properties calculated using this technique can be accurate in theory and the temperature range can span both solid and liquid phase range. The main disadvantage is that the computations are rather expensive and complicated. The complexity arises not only from the computational process itself but also from the needs that the convention *ab initio* code has to be modified to deal with the mixed interactions.

In this work we present a simple scheme to calculate the free energy, especially the intrinsic anharmonic term. This approach can reach nearly the same precision as the AITI method but with much less computation costs. Using W as a prototype, its thermodynamic properties were calculated. W is an important standard material whose equation of state (EOS) can be used as a pressure scale. The EOS of W has a very good consistency between static and dynamic pressure experiments at relatively high pressures and temperatures,¹⁴ which gives a small experimental uncertainty range of EOS. The thermodynamic properties of W have been calculated before by using a PIC-based method¹⁵ and two quasiharmonic-approximation-based methods.^{7,16} As mentioned above, the former neglected the vibrational correlations of the ions and the later two ignored the intrinsic anharmonic effect. So it is meaningful to perform the accurate calculations of the thermodynamic properties including thermal EOS of W by taking the intrinsic anharmonic effect into account.

In the following sections we shall first describe the basic theory of our scheme and then the details of thermal-property calculations of W. After that the calculated results are shown and compared with the experimental results, and some further thoughts on this method are followed. Finally a summary is given.

II. COMPUTATIONAL METHODS

A. Basic theory

For a system with a given volume V and temperature T , the Helmholtz free energy $F(V, T)$ usually can be decomposed into the sum of the following three independent terms:

$$F(V, T) = E_0(V) + F_e(V, T) + F_i(V, T), \quad (1)$$

where $E_0(V)$ is the total energy at 0 K with the fixed ionic positions, $F_e(V, T)$ is the thermal free energy from the electronic excitations, and $F_i(V, T)$ is the vibrational contribution of the ions to the free energy. The last part $F_i(V, T)$ can be further divided into the quasiharmonic contribution $F_q(V, T)$ and the intrinsic anharmonic contribution $F_a(V, T)$,

$$F_i(V, T) = F_q(V, T) + F_a(V, T). \quad (2)$$

Similar to the division of free energy to all these parts, all other quantities related to it, such as pressure and entropy, can also be separated to the corresponding term. Here after we shall use the similar subscripts to denote other corresponding quantities.

The sum of $E_0(V)$ and $F_e(V, T)$ as a whole part (static free energy F_s) can be calculated using DFT generalized to finite temperatures by the Mermin theorem.¹⁷ The quasiharmonic contribution $F_q(V, T)$, including the zero-point energy, can be obtained from the calculated phonon frequencies, ω_i , via the standard statistical thermodynamics formula,

$$F_q(V, T) = k_B T \sum_i \left\{ \frac{1}{2} x_i + \ln[1 - \exp(-x_i)] \right\}, \quad (3)$$

where $x_i = \hbar \omega_i / k_B T$, \hbar and k_B are Planck's constant and Boltzmann's constant, respectively, and the sum is over all the

normal modes. Note that here the phonon frequencies ω_i are not only a function of V , which is the case in the conventional quasiharmonic approximation but also a function of T simultaneously.

The full dispersion relations of phonon can be calculated by two types of methods: frozen phonon method and linear-response theory.¹ Here we choose the frozen phonon method. In this method one reference atom of the system is displaced for several small distances according to the symmetry from its equilibrium position and the forces felt by other atoms in the system are calculated, which are then used to determine the force constants in the so-called dynamical matrix. Finally the PDRs are obtained by diagonalizing the dynamical matrix.¹⁸ In real calculations of the force constants, supercells with the periodic boundary condition have to be used to simulate the infinite crystalline. Anyhow, the calculation of the quasiharmonic contribution F_q , compared to that of the intrinsic anharmonic contribution F_a , is straightforward and relatively cheap.

It is much more challenging to calculate F_a than F_q because there is no simple and direct formula like Eq. (3) to link the known quantities with those unknown quantities, although, as we shall see, F_a is relatively smaller and only becomes important at high temperature. Here we give an approximate formula to fulfill this task. According to classical statistical mechanics, the anharmonic free energy F_a is quadratic in temperature based on the lowest-order perturbation theory.¹⁹ This approximation is derived from the result of the expansion of the potential to fourth order. In general, this is enough accurate because the anharmonic contribution of solids is relatively small and the contribution from the higher order term is even smaller. Usually, solids have already melted or decomposed before the higher order term becomes important. Actually, this approximation that F_a goes as T^2 has already been used widely for the calculations of thermal properties of solids at temperatures up to their melting points.^{13,20} Besides this approximation, here we further assume that the volume dependence of F_a can be expressed approximately as a polynomial, thus

$$F_a(V, T) = (\alpha_0 + \alpha_1 V + \alpha_2 V^2 + \dots + \alpha_n V^n + \dots) T^2, \quad (4)$$

where $\alpha_0, \alpha_1, \alpha_2, \dots, \alpha_n$ are fitting parameters. Using this approximate function expression of $F_a(V, T)$ in Eq. (4) one can develop the following simple approach to calculate the anharmonic free energy.

Suppose we have two systems, system I and system II, both with the same volume V , temperature T , and number of particles N but with different interactions: system I with the ideal quasiharmonic interaction while system II with both the quasiharmonic and the anharmonic interactions. With the approximation in Eq. (4), simple deduction (see Appendix) results in a relation which links the free-energy difference with the total-energy (internal energy) difference of the two systems,

$$F_a = F_{II}(V, T) - F_I(V, T) = -[U_{II}(V, T) - U_I(V, T)], \quad (5)$$

where F_I and U_I are the free energy and the total energy of systems I, respectively, F_{II} and U_{II} of the systems II. This relation shows that the intrinsic anharmonic contribution F_a

can be obtained by directly calculating the total energy of systems I and II without using any intermediate states, which are indispensable in the AITI method.

The total energy of system I in Eq. (5) can be easily obtained from its relation with free energy, $U=F-T(\partial F/\partial T)$, after the static free energy F_s and the quasiharmonic free energy F_q are calculated, respectively. At the same time the total energy of system II can be measured directly in an AIMD simulation. After obtaining U_I and U_{II} , one can determine the parameters in anharmonic free energy F_a in Eq. (4) using Eq. (5). To be specifically, suppose there are only three parameters to be determined in Eq. (4) (that is, α_0 , α_1 , and α_2). In this case we need to calculate U_I and U_{II} in three independent states, then solve the equation sets made of Eq. (5) for the two systems in these three states. For the cases with more parameters than three ones, the process used to determine them is the same. The only difference is that the calculations for the two systems in more states are needed. We shall show that three-parameter description is sufficient for most of crystalline solids. After all these parameters are determined accurately, the anharmonic contribution $F_a(V,T)$ is completely determined. Till here all the terms in free energy $F(V,T)$ are known. With the known function $F(V,T)$, other thermal properties can be easily derived.

B. Calculation details for bcc W

All the present calculations were performed using Vienna *ab initio* simulation package,²¹ which is a plane-wave code for *ab initio* density-functional calculations. The projector-augmented-wave approach^{22,23} was used for describing the electron-ion interaction of W, and *5p*, *5d*, and *6s* orbitals were treated as valence states. The plane-wave cutoff energy was 300 eV. All the calculations were based on the same generalized-gradient approximations (GGAs) of exchange-correlation functional due to Perdew, Burke, and Ernzerhof,²⁴ except for the test case using local-density approximations (LDAs).²⁵ The spin-orbit interactions were found to have only a negligible effect on the EOS, so our computations were performed without taking the spin-orbit coupling interactions into account.

For the total-energy calculations using the primitive cells of bcc W (only one atom) at various electronic temperatures and atomic volumes, we used the $22 \times 22 \times 22$ *k*-point Monkhorst-Pack²⁶ mesh to sample the Brillouin zone. In order to obtain the accurate static pressure P_s (without ion vibrational contribution but with electronic temperature taken into account), we computed the total energies for up to 161 equally spaced atomic volumes ranging from 9.4105 to 21.4375 Å³ at the corresponding electronic temperatures including 0, 100, 300, and 600 K, and the range from 1000 to 10 000 K in 500 K increments. The energies at certain electronic temperature were then fitted to the fourth-order Birch EOS (Ref. 27) with its reduced form

$$E_0 + F_e = A_0 + A_1X + A_2X^2 + A_3X^3 + A_4X^4, \quad (6)$$

where $X=V^{-2/3}$ and A_0 , A_1 , A_2 , A_3 , and A_4 are the fitting parameters. The analytical derivative of Eq. (6) gives the static pressure P_s from E_0 and F_e as

$$P_s = \frac{2(A_1V^2 + 2A_2V^{4/3} + 3A_3V^{2/3} + 4A_4)}{3V^{11/3}}. \quad (7)$$

As mentioned above, in the calculation of the phonon-dispersion relations using the frozen phonon method, supercells have to be used. Except for the test case in which we use 125 atoms, all the supercells for force-constant calculations have 64 atoms and the displacement amplitude of the reference atom is 0.0141*a*, which changes with lattice constants *a*. For electronic *k*-point sampling, we used a $6 \times 6 \times 6$ *k*-point Monkhorst-Pack set, which reduces *k*-point errors to less than 0.1 meV/atom at all electronic temperatures of interest. Integration over the phonon Brillouin zone was performed using 770 Monkhorst-Pack *k* points in the irreducible wedge.

In order to obtain accurately the quasiharmonic free energy F_q as a function of *V* at a certain temperature, the F_q at ten equally spaced atomic volumes ranging from 9.4105 to 16.2065 Å³ have been calculated. The quasiharmonic free energies were fitted to fourth-order polynomial of *V* and the corresponding pressures were then analytically derived from the polynomial. Because the PDRs change not only with volumes but also with electronic temperatures, although the change with electronic temperature is relatively slow, we calculated the PDRs at electronic temperatures 300, 2000, 4000, 6000, 8000, and 10 000 K, respectively. At these temperatures the quasiharmonic free energy $F_q(V,T)$ and the related entropies and total energies are calculated from PDRs at the exact electronic temperatures. The quasiharmonic free energy at other temperatures was evaluated using the linear interpolations of the two free energies calculated from the two PDRs with electronic temperatures near the target electronic temperature. For example, the free energy at 7000 K is obtained from two free energies: one is evaluated using the PDRs at the electronic temperature 6000 K and the other one using the PDRs at the electronic temperature 8000 K, both at the same ion temperature of 7000 K. This is different from the directly interpolation of the two free energies, one at ion temperature of 6000 K with the PDRs at the corresponding electronic temperature of 6000 K and the other one at ion temperature of 8000 K with the PDRs at the corresponding electronic temperature of 8000 K.

The quasiharmonic free energy calculated from the PDRs are fitted to a fourth-order polynomial of the atomic volume at various temperatures as $F_q=D_0+D_1V+D_2V^2+D_3V^3+D_4V^4$, where D_0 , D_1 , D_2 , D_3 , and D_4 are fitting parameters. The pressure-volume relation at the corresponding temperature then can be represented as $P_q=-(D_1+2D_2V+3D_3V^2+4D_4V^3)$. It should be pointed out that there are no physical reasons for choosing polynomial to fit the *F-V* relations. Its reliability and accuracy depend on dense sampling along these curves. Here we sampled each curve with up to ten points along it while in the similar calculations for hcp iron only seven points for each curve were used.¹³ The advantage of our method is that we do not need to use any other approximations like special form of Grüneisen parameter used in those methods based on Mie-Grüneisen equation.²⁸

As mentioned above, to determine the intrinsic anharmonic free energy F_a , we only need to obtain all the parameters in Eq. (4). Here we used the two-parameter expression

for F_a , namely, $F_a = (\alpha_0 + \alpha_1 V)T^2$. We shall show later that the two-parameter expression is accurate enough for the thermodynamic description of W at high temperature. Actually the same two-parameter expression (with different parameter values) has already been shown to be able to express accurately the anharmonic term in the hexagonal-close-packed iron under Earth's core conditions.¹³ To determine the two parameters in F_a , here we used two methods: one was to solving the equation set of energy Eq. (5) of the two systems in two independent (V, T) states; and the other way was to obtain the two parameters by solving the equation set of the energy Eq. (5) and the pressure $P_a = -\alpha_1 T^2$ simultaneously of the two systems in only one (V, T) state. In the first method, we calculated the total energies for each system in two states: one with the atomic volume $V_1 = 9.4105 \text{ \AA}^3$ and temperature $T_1 = 10\,000 \text{ K}$, and the other with $V_2 = 10.1620 \text{ \AA}^3$ and $T_2 = 8000 \text{ K}$. The static total energies of system I in these two states were calculated at the corresponding electronic temperatures. At the same time, the total energies of system I from the phonon contributions in these two states were obtained from the PDRs in the corresponding states without using any interpolations. The total energies of system II in these two states were calculated directly from two constant-temperature AIMD simulations with Nosé-Hoover thermostat.^{29,30} The simulations were performed using the supercells with 128 atoms and only the Γ points were used for the electronic-structure calculations. In the second method, we calculated the total energy and pressure from the simulation performed for each system both in the first state (V_1, T_1) . The time step for the ion motion was set to 0.5 fs and the first 1000 steps were run for the system to reaching equilibrium and the following 500 steps were used for the properties statistics.

III. RESULTS AND DISCUSSION

In this section, first we show the results of the three parts of the free energy and some of the related quantities for bcc W. With all these data the EOSs at room temperature and in Hugoniot states are then presented. After that the linear thermal-expansion coefficient is compared with the experimental data. Finally some further thoughts about this method are given.

A. Static EOS and quasiharmonic contributions

To show the effect of electronic temperature on the EOS, in Fig. 1 we plotted the static pressure versus volume relation at 0 and 10 000 K. It is clear that the electron excitations play important roles in the static EOSs, especially for the system at low density (with large atomic volume).

Before we turn to the descriptions of quasiharmonic contributions to the EOS of W, we talk about some characteristic effects of volume and electronic temperature on the PDRs. The calculated PDRs (Fig. 2) in some special direction of the phonon Brillouin zone can reproduce closely the experimental data³¹ at zero pressure and 300 K. This shows partly that the calculated PDRs are reliable. In some materials, such as hcp iron,¹³ the PDRs at two different volumes can be ap-

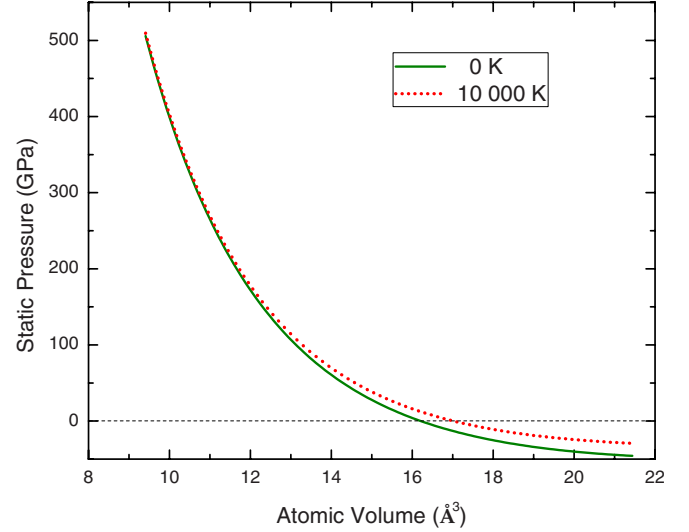


FIG. 1. (Color online) Static pressure (with all ions fixed) as a function of atomic volume at different electronic temperatures.

proximately scaled with one parameter. This is not the case for bcc W because the shape of the phonon-dispersion curve also changes notably with volumes, especially in some special directions, such as ΓH in Fig. 2. Along ΓH the frequency extremum in one of the phonon branches at the uncompressed state vanishes at the compressed state. Besides the volume effects on the PDRs, the raised temperature can also lead to a decline in phonon frequencies, although the temperature effects (Fig. 3) are relatively smaller compared to the volume effects on the PDRs. Similar to the volume effects on PDRs, it is also not able to scaled the phonon PDRs at two different temperatures with just one parameter. The phonon densities of states (DOSs) also show the prominent changes with both volume (Fig. 2) and temperature (Fig. 3).

The pressure-volume relations from the quasiharmonic contribution at some choosing temperatures are shown in

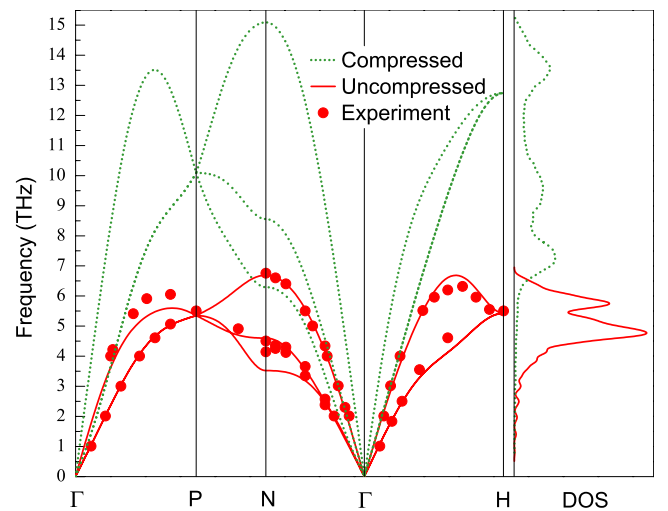


FIG. 2. (Color online) Volume effects on phonon-dispersion relations and phonon DOS at 300 K. The experimental data at $T = 296 \text{ K}$ and ambient pressure are taken from Ref. 31. The compressed and uncompressed states correspond with the atomic volume of 9.4105 and 16.2065 \AA^3 , respectively.

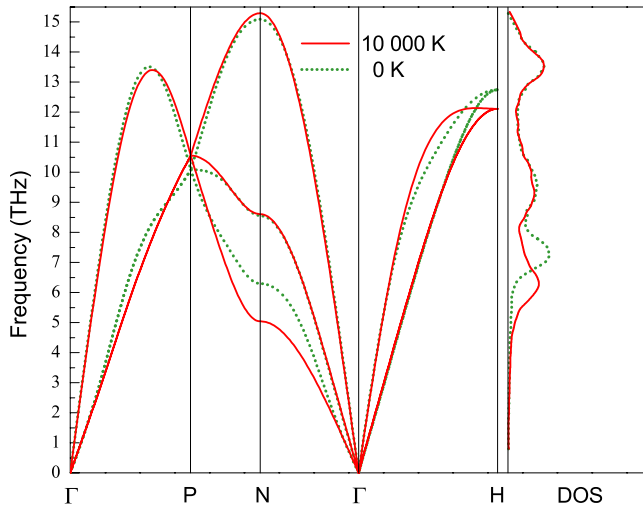


FIG. 3. (Color online) Electronic temperature effects on phonon-dispersion relations and phonon DOS at the small atomic volume of 9.4105 \AA^3 .

Fig. 4. It is quite clear that the changing tendencies of the pressure with volume are significantly different at different temperatures. The quasiharmonic pressure contributions at relatively low temperature change nonmonotonically with volume maybe results from the complicated nonlinear change in PDRs with volume.

B. Anharmonic contribution

Solving the equation set constructed using Eqs. (4) and (5) with the calculated static total energies and quasiharmonic total energies of system I in two states, (V_1, T_1) and (V_2, T_2) and the total energies measured from the two AIMD simulations for system II in the same two states, we obtained the final results for the two parameters in $F_a = (\alpha_0 + \alpha_1 V)T^2$, which are $\alpha_0 = 5.32 \times 10^{-9} \text{ eV K}^{-2}$ and $\alpha_1 = -6.56 \times 10^{-10} \text{ eV \AA}^{-3} \text{ K}^{-2}$ per atom. The second calculation method which used both the total energy and pressure in

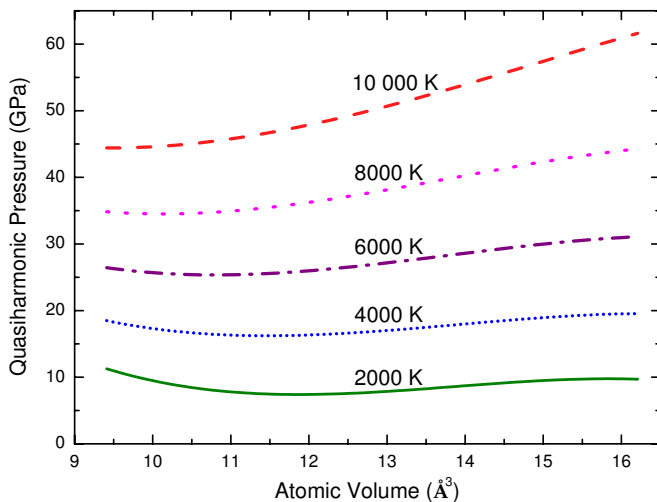


FIG. 4. (Color online) Quasiharmonic pressures as functions of the atomic volume at various temperatures.

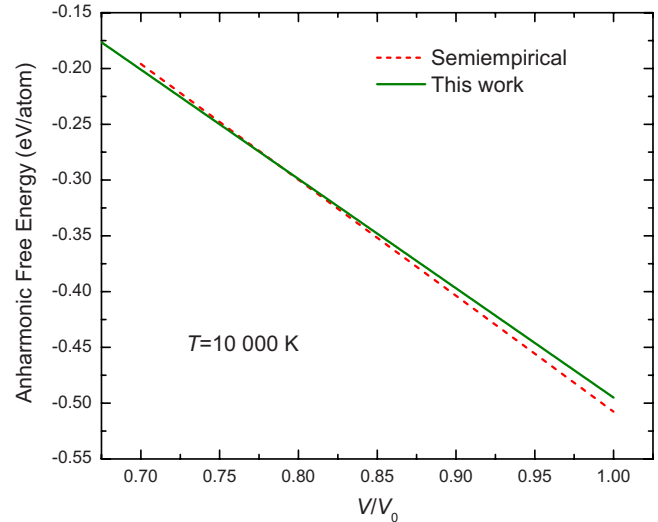


FIG. 5. (Color online) Anharmonic free energy as a function of the relative volume at 10 000 K. The semiempirical result is calculated using the model and parameters from Ref. 28.

(V_1, T_1) to determined the two parameters leads to only a slightly difference for the two parameters. Although in principle the calculations with only one states should take less time, we find that this method actually do not save time because the stress calculations in the AIMD simulations are time consuming, which are not needed in the first method.

The anharmonic free energy $F_a = (\alpha_0 + \alpha_1 V)T^2$ governed by these two parameters is relatively small compare to the quasiharmonic free energy. The ratio of F_a to F_i decreases with volume at a certain temperature. It reaches at most 5% at 10 000 K. The anharmonic free energy as a function of relative volume V/V_0 at 10 000 K are shown in Fig. 5. This result is very close to the one calculated using the semiempirical description of the same part with ten parameters.²⁸ The anharmonic pressure $P_a = -\alpha_1 T^2$ goes up to 10 GPa at 10 000 K and all volumes.

In our calculations we neglected the difference between the quantum calculations with zero-point vibrational effect involved in Eq. (3) and the classic calculations involved in the AIMD simulations without zero-point vibrational effect. This treatment is proper both at low and high temperatures. At low temperature the anharmonic free energies, which were calculated using the parameters determined using the states at relatively high temperatures, are small and can be neglected. At high temperature, zero-point vibrational effect is negligible.

C. Room-temperature EOS

At room temperature the anharmonic term in the free energy is very small and we do not need to include this part in the room-temperature EOS. In the EOS calculations of many metals GGA functionals are usually better than LDA ones but there do exists some exceptions such as Pt (Ref. 12) and Au (Ref. 16) for which the LDA functionals are better. To determine which functional is better, we show in Fig. 6 the comparison between the calculated the LDA and GGA pres-

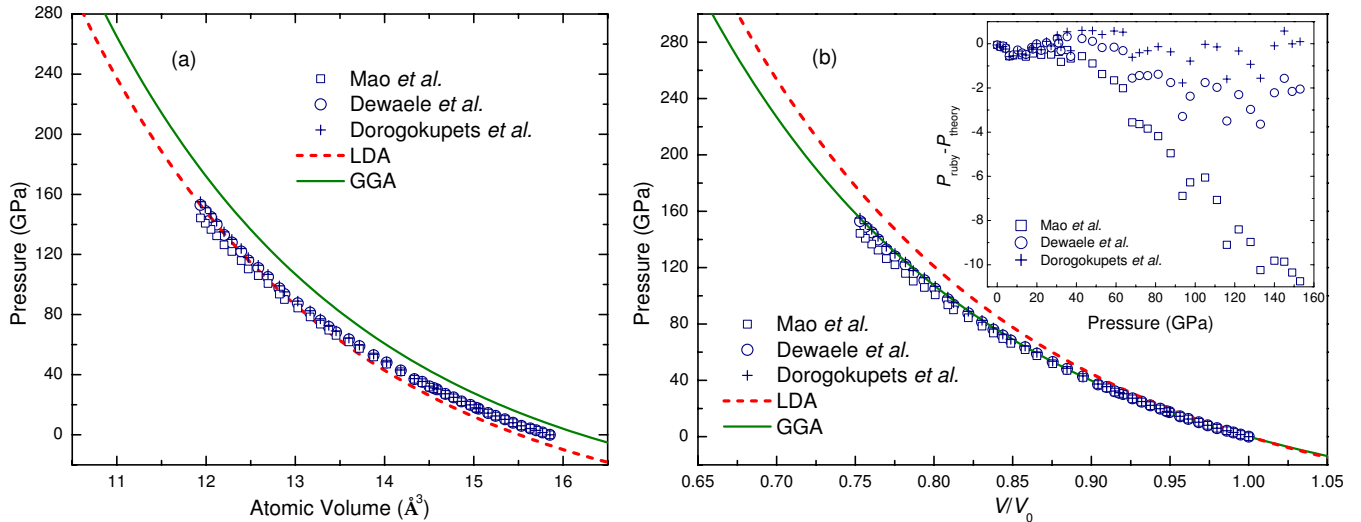


FIG. 6. (Color online) (a) Comparison between GGA and LDA pressures, as functions of the atomic volume and the experimental data of Dewaele *et al.* (Ref. 14) using the ruby pressure scales proposed by Mao *et al.* (Ref. 32), Dewaele *et al.* (Ref. 14), and Dorogokupets *et al.* (Ref. 28). (b) Similar comparison but with pressures as functions of the relative volume V/V_0 . The inset: difference between the data of Dewaele *et al.* (Ref. 14) using the three ruby scales (P_{ruby}) and the GGA pressures (P_{theory}) as functions of the GGA pressures. Note here V_0 is taken from the corresponding balanced volume of each calculational or experimental method: 16.25 \AA^3 for the GGA calculations, 15.50 \AA^3 (at 0 K) for the LDA calculations, and 15.85 \AA^3 for the experiments.

pressures and those measured in diamond-anvil cell at room temperature¹⁴ using the ruby pressure scales proposed by Mao *et al.*,³² Dewaele *et al.*,¹⁴ and Dorogokupets and Oganov.²⁸ Here both the LDA and GGA pressures from quasiharmonic contribution are calculated directly from the PDRs using GGA functional. From the pressure-volume relations shown in Fig. 6(a), it seems that the LDA calculational results are much closer to the experimental one. But if judging from the relation of the pressure versus relative volume V/V_0 shown in Fig. 6(b), the GGA calculations are much better. So in all our calculations the GGA functional is used except for this test case. The inset in Fig. 6(b) shows the difference between the pressures measured using the three pressure scales and the GGA pressures as functions of the GGA pressure. It is quite clear that our results are more close to the ones using the ruby pressure scales proposed by the Dorogokupets and Oganov.²⁸

Our GGA balanced atomic volume (16.25 \AA^3) at room temperature is almost the same as the one (16.26 \AA^3) calculated from the full potential linearized augmented plane wave method,¹⁵ which is thought to be more accurate because no pseudopotential is used. This shows partly that our GGA calculations are reliable.

D. Hugoniot EOS

To compare our results of the EOS of W at high compression and high temperatures with those derived from the shock data, we also calculated the pressures P_H and temperatures T_H on the Hugoniot for a set of relative volumes ranging from 0.675 to 0.925 \AA^3 by solving the Rankine-Hugoniot equation:³³ $P_H(V_0 - V) = 2(E_H - E_0)$, where E_H is internal energy along the Hugoniot, and E_0 and V_0 are, respectively, zero-pressure room-temperature energy and volume of the *ab initio* results. For a given volume V , the tem-

perature on the Hugoniot is varied until Rankine-Hugoniot equation is satisfied. The theoretical Hugoniot curves for W and the corresponding experimental data^{34,35} are shown in Fig. 7. Although there are enough P - V experimental data which are closely reproduced in our theoretical work, more temperature measurements are needed in Hugoniot states to check the calculation for temperature.

E. Linear thermal-expansion coefficient

The linear thermal-expansion coefficient can be obtained from the equation: $\alpha = (\partial V / \partial T)_P / 3V$. If the two-parameter model of anharmonic free energy is used, from a simple deduction we can find that its contribution to the linear thermal-expansion coefficient is exactly zero (not zero if the accurate descriptions need three or more parameters for some materials). This means that all thermal expansion will exclusively be contributed from the other two parts of the free energy: the quasiharmonic free energy and the static free energy. The anharmonic term mainly increases the pressure in the system and gives a small amount of pressure calibration. The calculated and experimental³⁶ linear thermal-expansion coefficients are shown in Fig. 8. The theoretical and experimental results are closely in agreement with each other.

F. Further thoughts

To gain some insights into the anharmonic free energy as a function of the volume at high temperatures, in Fig. 9 we plotted the anharmonic free energies of Au, Ag, Cu, Ta, MgO, and diamond as functions of the relative volumes at 10 000 K based on the semiempirical description of the anharmonic part of the free energy with ten parameters.²⁸ In order to keep the solids from melting, the real relative vol-

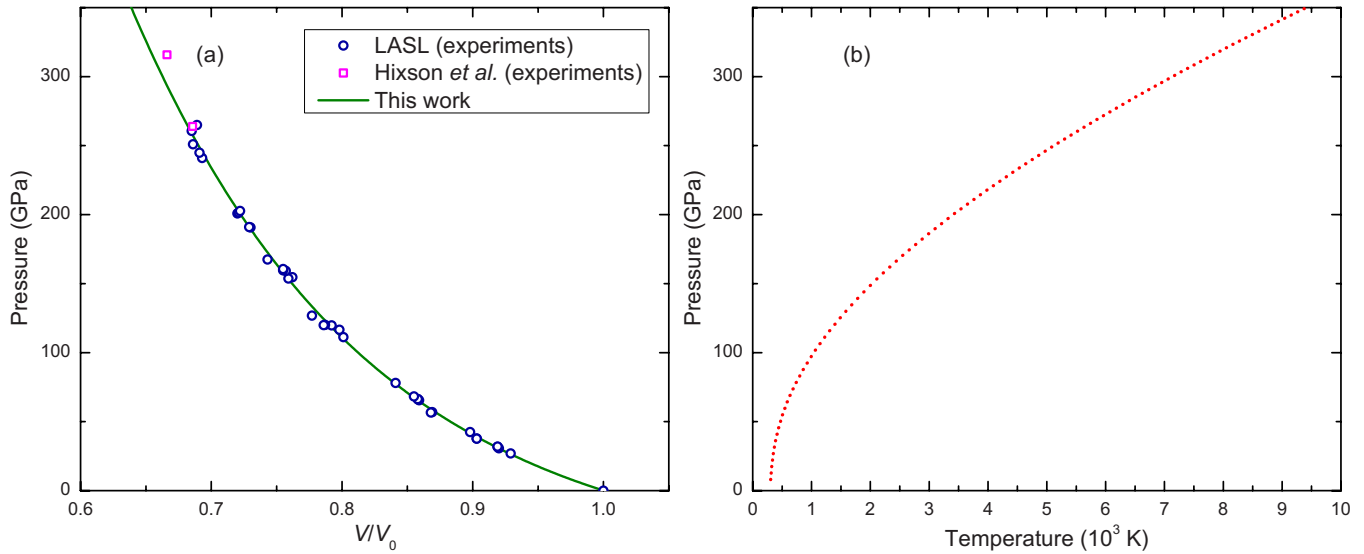


FIG. 7. (Color online) (a) Theoretical Hugoniot for W compared to experimental Hugoniot data taken from Ref. 34 (LASL) and Ref. 35 (Hixson *et al.*). (b) Theoretical temperatures along the Hugoniot.

ume actually is much less than that shown in Fig. 9. For these materials a second- or even first-order polynomial expression of the volume dependence of the anharmonic free energy is enough accurate. This shows that, in theory, the calculations performed in only three states are needed to determine completely the anharmonic free energy as a function of the volume and the temperature according to Eq. (4). This gives us the confidence that our method can work efficiently for a wide range of materials. On the other hand, the two- or three-parameter description of the anharmonic free energy of the form in Eq. (4) is simple but accurate and hence a widely use of the three-parameter model for all kinds of materials at high temperature is highly recommended.

To determine the parameters in the anharmonic free energy with a high precision using the calculation results performed in fewer states, the AIMD simulations should be per-

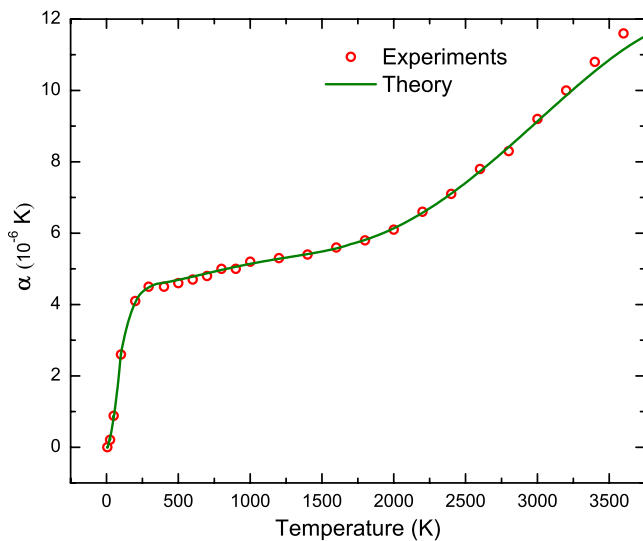


FIG. 8. (Color online) Comparison between the calculated linear-expansion coefficient of W at ambient pressure and the experimental data taken from Ref. 36.

formed at the temperature as high as possible (of course melting is not allowed). In these states the anharmonic contributions are large and the errors can be decreased to the lowest level. Another way to increase the precision is to perform the AIMD simulations in the states with large volume difference and each volume should be as large as possible. With these considerations, the calculations of the free energy using our method can be as accurate as the AITI method but with much less cost.

As already mentioned above, our method can work both at low temperature and relatively high temperature (lower than melting point), this is significantly better than those

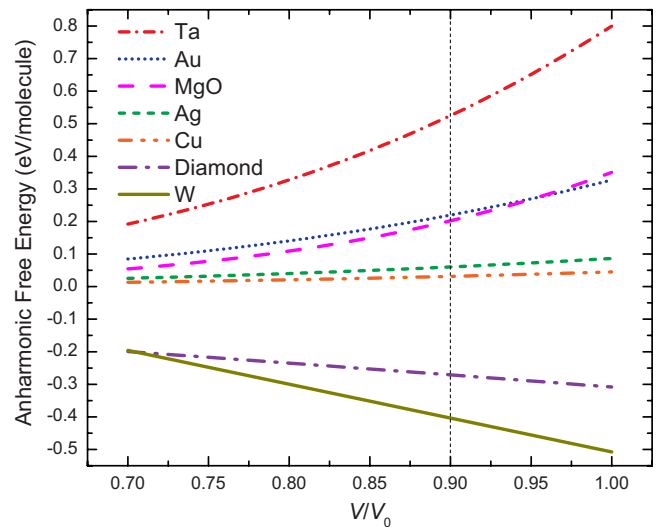


FIG. 9. (Color online) The anharmonic free energies of various materials as functions of their relative volume V/V_0 at 10 000 K. The data are evaluated from the parameterized semiempirical formulation of anharmonic free energy in Ref. 28. The vertical dashed line at $V/V_0=0.9$ is to show schematically that the relative volume for a solid keep its solid phase at 10 000 K is usually lower than this value.

TABLE I. Relative volume (V/V_0) as a function of pressure (in GPa) and temperature (K). Here V_0 is the calculated volume (16.25 \AA^3) at zero pressure and room temperature.

P	300	600	1000	1500	2000	2500	3000
10	0.9699	0.9757	0.9800	0.9888	0.9999	1.0106	1.0176
20	0.9436	0.9485	0.9523	0.9597	0.9691	0.9784	0.9843
30	0.9204	0.9246	0.9278	0.9342	0.9423	0.9502	0.9554
40	0.8996	0.9032	0.9061	0.9117	0.9186	0.9254	0.9301
50	0.8810	0.8840	0.8866	0.8916	0.8976	0.9034	0.9077
60	0.8640	0.8666	0.8690	0.8735	0.8787	0.8838	0.8877
70	0.8485	0.8508	0.8529	0.8570	0.8616	0.8661	0.8697
80	0.8342	0.8362	0.8381	0.8419	0.8460	0.8499	0.8533
90	0.8210	0.8227	0.8245	0.8279	0.8316	0.8351	0.8383
100	0.8087	0.8102	0.8118	0.8150	0.8183	0.8215	0.8245
110	0.7971	0.7985	0.8000	0.8030	0.8060	0.8089	0.8117
120	0.7863	0.7875	0.7890	0.7917	0.7945	0.7972	0.7998
130	0.7761	0.7772	0.7786	0.7812	0.7837	0.7862	0.7886
140	0.7665	0.7675	0.7688	0.7712	0.7736	0.7758	0.7782
150	0.7574	0.7583	0.7595	0.7618	0.7640	0.7661	0.7683
160	0.7487	0.7496	0.7508	0.7529	0.7550	0.7569	0.7590
170	0.7405	0.7413	0.7424	0.7444	0.7464	0.7482	0.7502
180	0.7326	0.7334	0.7345	0.7364	0.7382	0.7400	0.7419
190	0.7251	0.7259	0.7269	0.7287	0.7304	0.7321	0.7339
200	0.7179	0.7186	0.7196	0.7213	0.7230	0.7246	0.7263
210	0.7110	0.7117	0.7126	0.7143	0.7159	0.7174	0.7190
220	0.7044	0.7051	0.7059	0.7075	0.7090	0.7105	0.7120
230	0.6980	0.6987	0.6995	0.7010	0.7025	0.7039	0.7054
240	0.6919	0.6925	0.6933	0.6948	0.6962	0.6975	0.6989
250	0.6859	0.6866	0.6874	0.6887	0.6901	0.6914	0.6928
260	0.6802	0.6809	0.6816	0.6829	0.6842	0.6855	0.6868
270	0.6747	0.6753	0.6761	0.6773	0.6786	0.6798	0.6811
280	0.6693	0.6700	0.6707	0.6719	0.6731	0.6743	0.6755
290	0.6641	0.6648	0.6655	0.6666	0.6678	0.6690	0.6702
300	0.6591	0.6598	0.6604	0.6615	0.6627	0.6639	0.6650

PIC-based methods, which are only fit for the properties calculations at high temperatures and thus result in a discontinuity description of thermodynamic properties. Because of the simplicity and high accuracy of this method, we think it is not only suited for the thermal-property calculations of different crystalline solids but also can be used to the study of the solid-solid phase transitions including those occur in some alloys. Although it cannot be used to calculate the free energy of liquids directly in the present forms, this method combined with the AITI method for liquids can still be useful for the study of the solid-liquid phase transitions.

IV. SUMMARY

In this work we present an accurate but relatively simple scheme to compute the thermodynamical properties of various crystalline solids in a wide range of pressure and temperature based on *ab initio* calculations. Compared to the AITI method, this approach can reduce the computation

costs without decreasing the calculation accuracy. Using W as an example, we have shown that its thermal properties such as the linear thermal-expansion coefficient and EOSs at high pressures and temperatures can be calculated accurately. For anticipated further use of the EOSs of W, in Appendix we tabulate the relative volume V/V_0 as a function of the pressure P and the temperature T in Table I, for the pressure up to about 300 GPa and temperature to 3000 K.

ACKNOWLEDGMENTS

This work was supported by the National Natural Science Foundation of China [Grants No. 108074158, No. 10776029/A06 (NSAF), and No. 10676034 (NSAF)], the Research Foundation of the National Key Laboratory of Shock Wave and Detonation Physics (Grants No. 9140C6702030802, No. 9140C6703010803, and No. 9140C6703010703), and the Development Foundation of CAEP (Grant No. 2008A0101001).

APPENDIX

Here we give a simple deduction of Eq. (5). Suppose system I denotes the quasiharmonic vibrational system and system II is the real system with both quasiharmonic and anharmonic interactions. According to the thermodynamic relation between free energy and total energy (internal energy), we have

$$F_a = F_{II} - F_I = (U_{II} - TS_{II}) - (U_I - TS_I) = (U_{II} - U_I) - T(S_{II} - S_I). \quad (\text{A1})$$

The entropy difference $S_{II} - S_I$ in Eq. (A1) can be related to free energy as

$$S_{II} - S_I = -(\partial F_{II}/\partial T)_V + (\partial F_I/\partial T)_V = -[\partial(F_{II} - F_I)/\partial T]_V = -[\partial F_a/\partial T]_V. \quad (\text{A2})$$

From the assumption of $F_a = (\alpha_0 + \alpha_1 V + \alpha_2 V^2 + \dots + \alpha_n V^n$

$+ \dots)T^2$, the partial derivative in Eq. (A2) can be written as

$$S_{II} - S_I = -[\partial F_a/\partial T]_V = -2(\alpha_0 + \alpha_1 V + \alpha_2 V^2 + \dots + \alpha_n V^n + \dots)T. \quad (\text{A3})$$

Substitute Eq. (A3) into Eq. (A1), we have

$$F_a = (U_{II} - U_I) + 2(\alpha_0 + \alpha_1 V + \alpha_2 V^2 + \dots + \alpha_n V^n + \dots)T^2 = (U_{II} - U_I) + 2F_a. \quad (\text{A4})$$

Simplify Eq. (A4), we finally obtain the relation in Eq. (5), which links the free-energy difference (anharmonic free energy) of the two systems to their total-energy difference. From the deduction process, one can find that the relation in Eq. (5) is the direct result of quadratic temperature dependence of F_a , no matter what forms of the volume dependence take.

*skxiang@caep.ac.cn

¹R. M. Martin, *Electronic Structure: Basic Theory and Practical Methods* (Cambridge University Press, Cambridge, 2004).

²S. Baroni, S. de Gironcoli, A. dal Corso, and P. Giannozzi, *Rev. Mod. Phys.* **73**, 515 (2001).

³A. C. Holt and M. Ross, *Phys. Rev. B* **1**, 2700 (1970).

⁴K. Westera and E. R. Cowley, *Phys. Rev. B* **11**, 4008 (1975).

⁵G. A. de Wijs, G. Kresse, and M. J. Gillan, *Phys. Rev. B* **57**, 8223 (1998).

⁶D. Alfè, M. J. Gillan, and G. D. Price, *Nature (London)* **401**, 462 (1999).

⁷A. Debernardi, M. Alouani, and H. Dreyssé, *Phys. Rev. B* **63**, 064305 (2001).

⁸J. Xie, S. P. Chen, J. S. Tse, S. de Gironcoli, and S. Baroni, *Phys. Rev. B* **60**, 9444 (1999).

⁹D. Antonangeli, M. Krisch, D. L. Farber, D. G. Ruddle, and G. Fiquet, *Phys. Rev. Lett.* **100**, 085501 (2008).

¹⁰E. Wasserman, L. Stixrude, and R. E. Cohen, *Phys. Rev. B* **53**, 8296 (1996).

¹¹S. Xiang, L. Cai, F. Jing, and S. Wang, *Phys. Rev. B* **70**, 174102 (2004).

¹²S. Xiang, L. Cai, Y. Bi, F. Jing, and S. Wang, *Phys. Rev. B* **72**, 184102 (2005).

¹³D. Alfè, G. D. Price, and M. J. Gillan, *Phys. Rev. B* **64**, 045123 (2001).

¹⁴A. Dewaele, P. Loubeyre, and M. Mezouar, *Phys. Rev. B* **70**, 094112 (2004).

¹⁵Y. Wang, D. Chen, and X. Zhang, *Phys. Rev. Lett.* **84**, 3220 (2000).

¹⁶C. Bercegeay and S. Bernard, *Phys. Rev. B* **72**, 214101 (2005).

¹⁷N. D. Mermin, *Phys. Rev.* **137**, A1441 (1965).

¹⁸M. Born and K. Huang, *Dynamical Theory of Crystal Lattices* (Oxford University Press, New York, 1954).

¹⁹L. D. Landau and E. M. Lifshitz, *Statistical Physics (Part I)*, Course of Theoretical Physics Vol. 5 (Pergamon, Oxford, 1980).

²⁰A. R. Oganov and P. I. Dorogokupets, *Phys. Rev. B* **67**, 224110 (2003).

²¹G. Kresse and J. Furthmüller, *Phys. Rev. B* **54**, 11169 (1996).

²²P. E. Blöchl, *Phys. Rev. B* **50**, 17953 (1994).

²³G. Kresse and D. Joubert, *Phys. Rev. B* **59**, 1758 (1999).

²⁴J. P. Perdew, K. Burke, and M. Ernzerhof, *Phys. Rev. Lett.* **77**, 3865 (1996).

²⁵D. M. Ceperley and B. J. Alder, *Phys. Rev. Lett.* **45**, 566 (1980).

²⁶H. J. Monkhorst and J. D. Pack, *Phys. Rev. B* **13**, 5188 (1976).

²⁷F. Birch, *J. Geophys. Res.* **83**, 1257 (1978).

²⁸P. I. Dorogokupets and A. R. Oganov, *Phys. Rev. B* **75**, 024115 (2007).

²⁹S. Nosé, *Mol. Phys.* **52**, 255 (1984).

³⁰W. G. Hoover, *Phys. Rev. A* **31**, 1695 (1985).

³¹*Numerical Data and Functional Relationships in Science and Technology*, edited by K. H. Hellwege and J. L. Olsen (Springer-Verlag, Berlin, 1981).

³²H. K. Mao, J. Xu, and P. M. Bell, *J. Geophys. Res.* **91**, 4673 (1986).

³³M. A. Meyers, *Dynamic Behavior of Materials* (John Wiley & Sons, New York, 1994).

³⁴*LASL Shock Hugoniot Data*, edited by S. P. Marsh (University of California Press, Berkeley, Los Angeles, 1980).

³⁵R. S. Hixson and J. N. Fritz, *J. Appl. Phys.* **71**, 1721 (1992).

³⁶Y. S. Touloukian, R. K. Kirby, R. E. Taylor, and P. D. Desai, *Thermal Expansion: Metallic Elements and Alloys*, Thermophysical Properties of Matter Vol. 12 (Plenum, New York, 1975).